Ocean Wave Modelling in Cempi Bay, West Nusa Tenggara during Northwest and Southeast Monsoon

ISSN: 2714-8726

Esa Fajar Hidayat^{1*}, Muchammad Iqbal Havis², Agustinus Sembiring², Karizma Fahlevy², Faizal Ade Rahmahuddin Abdullah³

¹Department of Marine Science, Faculty of Fisheries and Marine Sciences, Brawijaya University
Jl. Veteran Malang, Jawa Timur 65145 Indonesia

²PT Lorax Indonesia

JL. Dr Ide Anak Agung Gde Agung Lot 5.1, Gedung Menara Rajawali Lt. 22, Kawasan Mega Kuningan, South Jakarta,
DKI Jakarta, 12950, Indonesia

³Faculty of Earth Sciences and Technology, Bandung Institute of Technology
Jl. Ganesa 10, Bandung, Jawa Barat, Indonesia

Email: *esafajarh21@ub.ac.id

Abstract

Coastal regions in Indonesia, such as Cempi Bay in West Nusa Tenggara, are strongly influenced by seasonal monsoon systems, which significantly affect wave dynamics and coastal processes. As the Northwest Monsoon (NWM) and Southeast Monsoon (SEM) exert non-uniform effects along Indonesia's coastline, accurate wave modeling is essential to support coastal management, fisheries, and disaster mitigation in this area. This study applies a numerical wave model driven by monsoonal wind data, supplemented with bathymetry and openboundary conditions, to simulate and analyze ocean wave characteristics in Cempi Bay during the NWM and SEM periods, focusing on significant wave height (H_s) and dominant wave period (T_p). Model performance was evaluated using Mean Absolute Percentage Error (MAPE), correlation coefficient (R), and Root Mean Square Error (RMSE). During NWM, H_s achieved a MAPE of 15.49%, R = 0.55, and RMSE = 0.19 m, indicating good agreement, while the initial SEM run showed a high MAPE of 42.83% for H_s that improved to 20.16% after scaling the H_s input by 79%, reducing the RMSE from 0.48 m to 0.26 m and increasing R from 0.67 to 0.68. Spatial analysis revealed distinct wave propagation patterns between the monsoons and confirmed lower wave energy in the inner part of Cempi Bay, highlighting the importance of capturing seasonal wave variability for effective coastal infrastructure planning and monsoon-adapted management strategies.

Keywords: Cempi Bay, wave modeling, ADCP, seasonal monsoon, numerical simulation

INTRODUCTION

Understanding the spatial and temporal dynamics of ocean waves is essential for effective coastal management, hazard mitigation, and marine infrastructure planning. Numerical wave modeling, when combined with observational data and validated against field measurements, provides a robust framework for analyzing wave characteristics in various coastal environments. In recent years, the application of numerical models such as Delft3D has grown significantly in Indonesia, driven by increasing concerns over coastal vulnerability and marine resource utilization (Handiani *et al.*, 2022; Harahap *et al.*, 2025; Sagala *et al.*, 2024). This study focuses on Cempi Bay, a semi-enclosed bay in West Nusa Tenggara that faces the Indian Ocean located in Dompu Regency in the south of Sumbawa Island. The bay covers four sub-districts of Pajo, Woja, Hu'u and Dompu and has an area of approximately 39,000 ha between latitudes 8°36'26.07"S – 8°53'6.08"S and longtitudes 118°7'35.64"E – 118°26'43.76"E. The bay is influenced by seasonal monsoonal wind patterns and large swell generated from the southern hemisphere. These factors contribute to complex wave behavior that requires detailed assessment. To characterize the seasonal wave conditions in Cempi Bay, this study applies the Delft3D-WAVE model using ERA5 reanalysis wind and wave data as boundary conditions, along with bathymetry data acquired from field surveys. Model outputs are then validated using in-situ Acoustic Doppler Current Profiler (ADCP) wave measurements to assess accuracy and model performance.

Previous studies have successfully employed Delft3D for wave modeling in various coastal settings across Indonesia and generally focused on open seas or major straits, with limited attention to semi-enclosed bays like Cempi Bay, which have complex bathymetry, monsoon-affected, and localized wind-wave

https://ejournal2.undip.ac.id/index.php/ijoce
DI: 10.14710/ijoce.v7i4.29242
DOI: 10.14710/ijoce.v7i4.29242
Disetujui/Accepted: 05-10-2025

interactions. A seasonal model of dynamics wave in Payangan Beach, Jember, using Delft3D-WAVE and ERA5 forcing, capturing significant wave height variability between calm and stormy conditions (Baresi *et al.*, 2023). Similarly, a coupled Delft3D-FLOW and WAVE simulation for Bedono Coast, Central Java, utilizing nested grids and validating the model with in-situ tidal and wave data (Mustaqim *et al.*, 2022). These studies highlight the reliability of Delft3D in simulating regional wave behavior and inform the methodological approach of the present work.

Despite its socio-economic importance, Cempi Bay has received little focused scientific attention. This semi-enclosed bay faces the open Indian Ocean and is directly exposed to seasonal monsoon systems, creating complex and highly variable wave conditions. These conditions influence fisheries, navigation routes, and coastal communities that are vulnerable to storm surges and extreme waves. Previous studies of monsoon-driven wave climates in Indonesia have largely concentrated on broader regional scales or open-coast settings, leaving the unique hydrodynamic characteristics of semi-enclosed bays like Cempi Bay insufficiently explored. Consequently, a clear understanding of the seasonal differences between the Northwest and Southeast Monsoons, and the quantitative performance of wave models under these conditions is still lacking. This knowledge gap limits the ability to design accurate coastal management strategies for fisheries activity, navigation safety, and disaster mitigation in Cempi Bay.

The objective of this study is to characterize the seasonal wave climate of Cempi Bay through numerical modeling supported by field measurements and secondary open-access data. By focusing on a semi-enclosed bay with direct exposure to open-ocean swell, the findings provide new insights into the hydrodynamic environment of such settings and offer a reference for future coastal development and marine spatial planning in the region.

MATERIALS AND METHODS

Wave Measurement Data

The Seabed mounted Teledyne ADCP (Workhorse Sentinel) - 1200 kHz was used for the wave measurements at an approximate water depth of 20 m. The wave measurement location is shown in Figure 1. The wave data were available for February and July 2023 at ADCP Station. The data from February represents the Northwest monsoon (NWM) while the data in July represents the Southeast monsoon (SEM). The wave measurements at ADCP station were obtained in the top bin with 2-hour interval in February and 4-hours interval in July. Measurements of wave heights and periods were conducted using a pressure sensor mounted in the ADCP. From the wave frequency spectra data, total wave energy can be calculated and used to estimate significant wave height $(H_{\rm S})$, peak wave period $(T_{\rm D})$ and mean wave direction $(D_{\rm m})$.

 H_s is defined as the average height of the largest 33% of waves sampled during a given period (Bitner-Gregersen & Magnusson, 2014; De Carlo & Ardhuin, 2024). This parameter emphasizes the larger, more "significant" waves and provides a better representation of prevailing wave conditions than smaller waves. The measured H_s values are presented seasonally using histograms. The peak wave period (T_p) , which represents the time interval between successive wave crests and corresponds to the most energetic waves in the total wave spectrum at a specific location, is also shown in histograms. The mean wave direction (D_m) denotes the average wave approach direction over a defined sampling period, which in this study is a 4-hour interval. T_p is shown together with H_s in the wave rose diagram, which illustrates the directional distribution of H_s across eight directional sectors.

Wave Propagation Model Setting

The Delft3D-WAVE numerical model was implemented within a computational grid spanning ~4,400km², with a corresponding length of ~74 km and width of ~86 km that nested to the wider grid of 20,700 km², with ~151 km length and ~164 km width (Figure 2). The selection of this domain extent was considered based on the data source location at 117.5° E for the West boundary, at 10.0° S for the South boundary, and at 119° E for the East boundary. Furthermore, the bathymetric information employed in this study was derived from field survey referenced to Mean Sea Level (MSL) supplemented with GEBCO 15 arc-seconds gridded bathymetry data, as visually represented in Figure 2 (right panel).

The domain was discretized using a rectangular grid to accurately represent the bathymetry. The evaluation was performed for a month of simulation for each season based on the availability of the field wave

Diterima/Received: 28-08-2025 Disetujui/Accepted: 05-10-2025

ISSN: 2714-8726

ISSN: 2714-8726

data. A time step of 1 minute is applied during the simulation. Physical input parameters adhered to recommended settings, including a activated refraction and diffraction process with uniform bottom friction coefficient of 0.067 m²/s³. Additionally, gravitational acceleration was set to 9.81 m/s², and sea water density to 1,025 kg/m³.

The wave that been evaluated in this study was sourced from the ECMWF-ERA 5 reanalysis dataset, representing the latest generation of ERA-5 data. These data are designated for evaluation and subsequent integration as input for as a space-varying wave boundary. The waves input boundary from ECMWF-ERA 5 consists of the hourly significant wave height combined wind waves and swell (SWH), peak period (PP1D), and mean wave direction (MWD). During the NWM and SEM simulation, the space-varying wave boundaries are applied at the West, the East and the South, with the interval of 0.5°.

The Delft3D-WAVE output was compared to measured wave data at a designated ADCP station in order to validate the model. This evaluation involved calculating the Mean Absolute Percentage Error (MAPE), along with considering the established correlation coefficient (*R*) and Root Mean Square Error (RMSE) (Williams & Esteves, 2017). An ideal correlation, indicating a perfect linear relationship, is represented by an *R*-value of 1. A positive *R*-value signifies a consistent, direct correlation, where both variables increase or decrease in tandem. Conversely, a negative *R*-value indicates an inverse or opposite correlation, meaning that as one variable increases, the other tends to decrease.

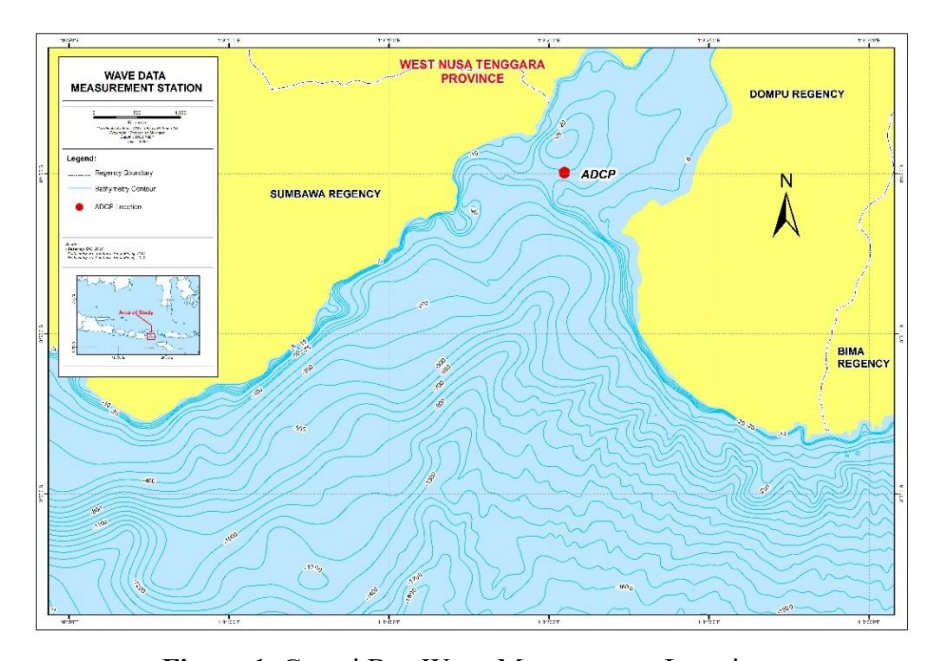


Figure 1. Cempi Bay Wave Measurement Locations

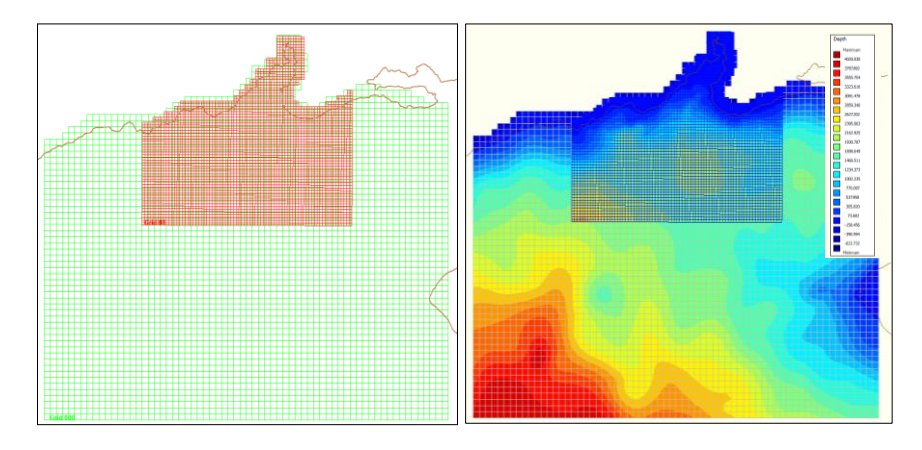


Figure 2. Cempi Bay Wave Modelling Nested Domain (left) and Bathymetry Grid (right)

Diterima/Received: 28-08-2025 Disetujui/Accepted: 05-10-2025

ISSN: 2714-8726

MAPE is calculated as the percentage of the absolute error between the comparative (x_0) and simulated (x_1) data (Adytia et al., 2023). According to Heizer and Render (2015), criteria for interpreting MAPE is as follows: MAPE <10% is excellent, 10-20% is good, 20-50% is moderate, and >50% is poor.

$$MAPE = \frac{1}{n} \sum \left(\frac{|x_0 - x_1|}{x_0} \right) \times 100\% \tag{1}$$

$$RMSE = \sqrt{\frac{\sum (x_0 - x_1)^2}{n}}$$

$$R = \frac{\sum (x_0 - \overline{x_0})(h_1 - \overline{x_1})}{\sqrt{\sum (x_0 - \overline{x_0})^2 \sum (x_1 - \overline{x_1})^2}}$$
(2)

$$R = \frac{\sum (x_0 - \overline{x_0})(h_1 - \overline{x_1})}{\sqrt{\sum (x_0 - \overline{x_0})^2 \sum (x_1 - \overline{x_1})^2}}$$
(3)

RESULT AND DISCUSSION

Model Validation

Before analyzing the seasonal wave climate, the Delft3D-WAVE model was validated against ADCP observations at Cempi Bay for February (NWM) and July (SEM). Model performance metrics for H_s , T_p , and D_m are summarized in Table 1. The time-series plots (Figures 3–5) show that the model captures the temporal variability of both monsoon seasons reasonably well. For H_s , the model achieved good skill during NWM (MAPE 15.5%, R=0.55) but initially overestimated during SEM (MAPE 42.8%, R=0.67). T_p showed better agreement during SEM (MAPE 14.4%, R=0.67) than NWM (MAPE 22.7%, R=0.48). D_m exhibited modest skill during SEM (R=0.48) but very weak correlation during NWM due to low directional variability.

To reduce SEM overestimation, the boundary H_s was scaled to 79% of its initial input, which improved model performance to MAPE 20.2%, RMSE 0.26 m, and R 0.68 (Figure 4c). This confirms that the calibrated model can reliably simulate wave conditions at Cempi Bay under both monsoon regimes.

Table 1. Wave model validation for H_s , $H_{s79\%}$, T_p , and D_m

Parameter/Season		MAPE (%)	R	RMSE
H_{S}	NWM	15.49	0.55	0.19 m
	SEM	42.83	0.67	0.48 m
$H_{s^{79\%}}$	SEM	20.16	0.68	0.26 m
T_p	NWM	22.74	0.48	3.14 s
	SEM	14.42	0.67	2.44 s
D_m	NWM	6.42	0.04	17.34°
	SEM	11.87	0.48	27.74°

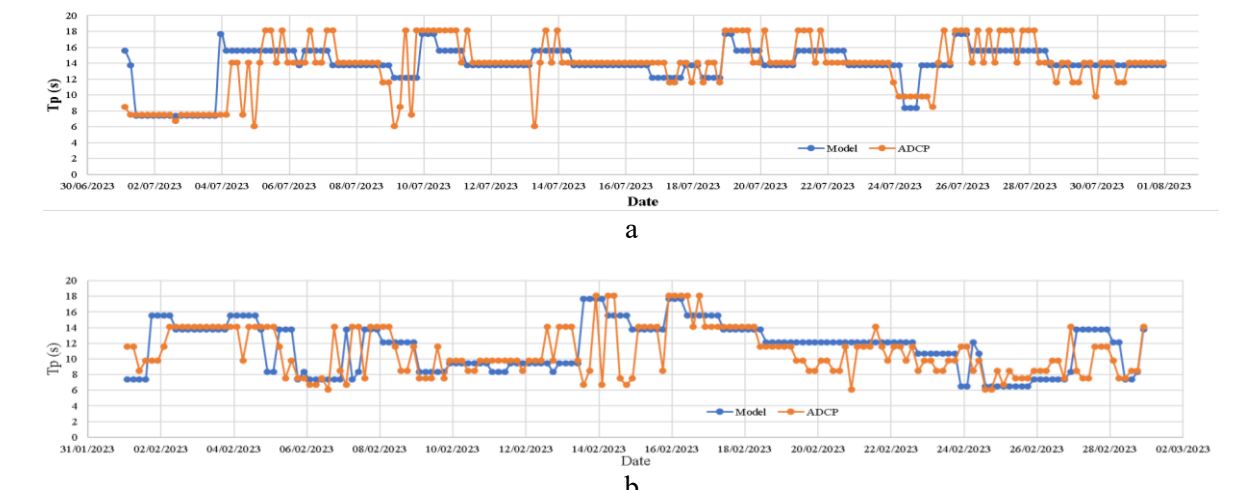


Figure 3. Time-series validation of T_p between the model and ADCP measurements during (a) the Northwest Monsoon (NWM) and (b) the Southeast Monsoon (SEM)

Diterima/Received: 28-08-2025 Disetujui/Accepted: 05-10-2025

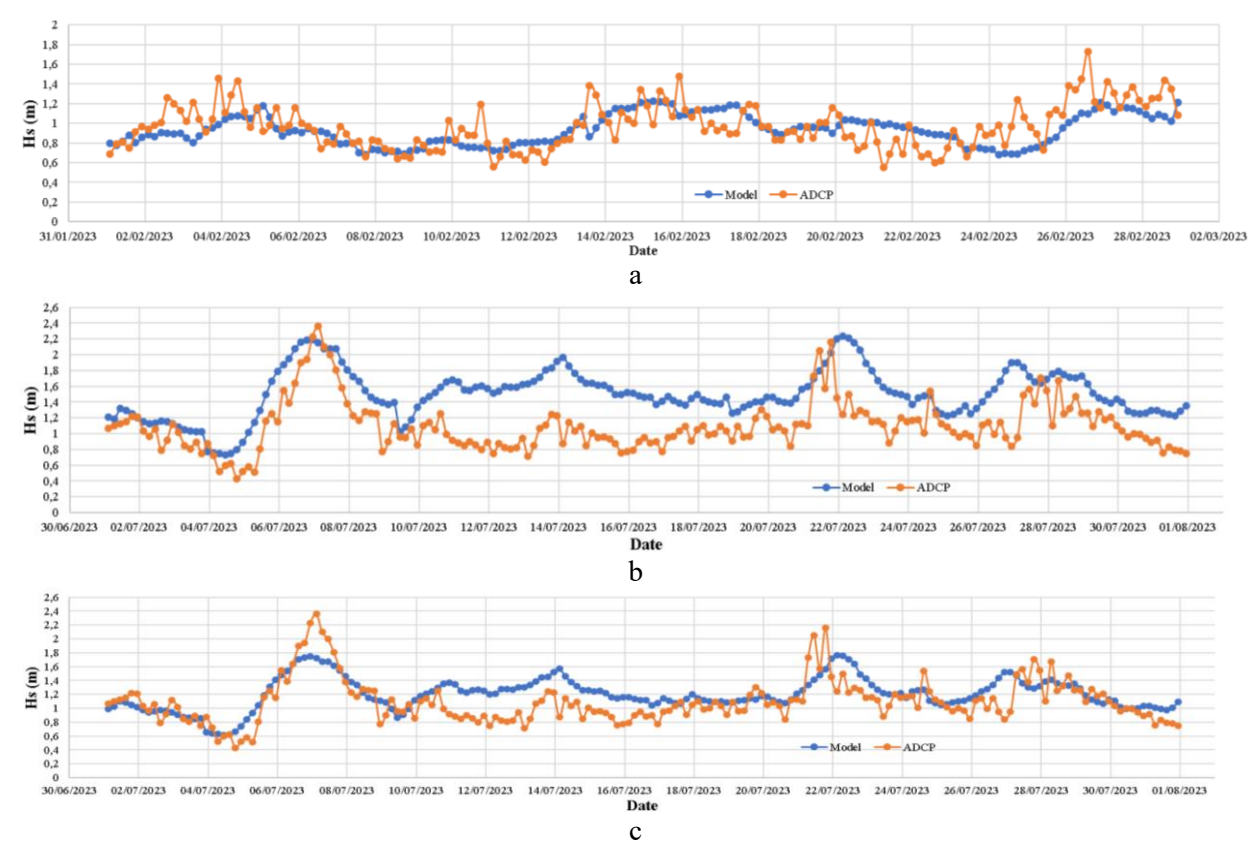


Figure 4. Time-series validation of H_s between the model and ADCP measurements during (a) the Northwest Monsoon (NWM), (b) the Southeast Monsoon (SEM), and (c) the SEM scenario with 79% scaleddown H_s

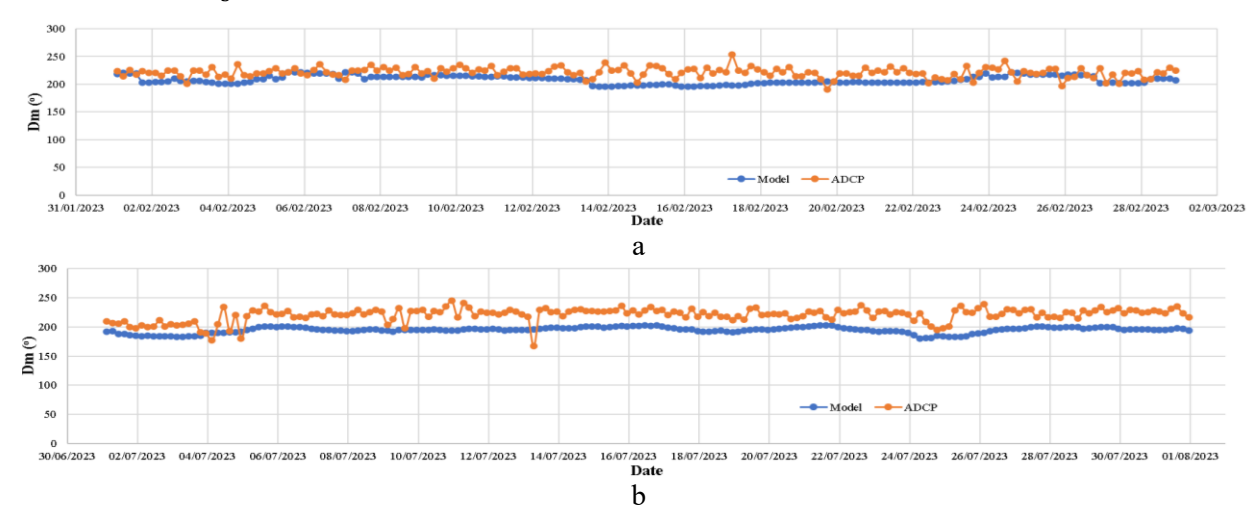


Figure 5. Time-series validation of D_m between the model and ADCP measurements during (a) the Northwest Monsoon (NWM) and (b) the Southeast Monsoon (SEM)

Seasonal Wave Characteristics at Cempi Bay Significant wave height

During the Northwest Monsoon (NWM), H_s recorded by the ADCP ranged from 0.55 m to 1.73 m, with an average of 0.97 m. The seasonal histogram (Figure 6a) shows that the majority of waves fell in the 0.5–1.0 m bin (59%), followed by 1.0-1.5 m (41%), and only a negligible fraction exceeded 1.5 m.

https://ejournal2.undip.ac.id/index.php/ijoce Diterima/Received: 28-08-2025 Disetujui/Accepted: 05-10-2025

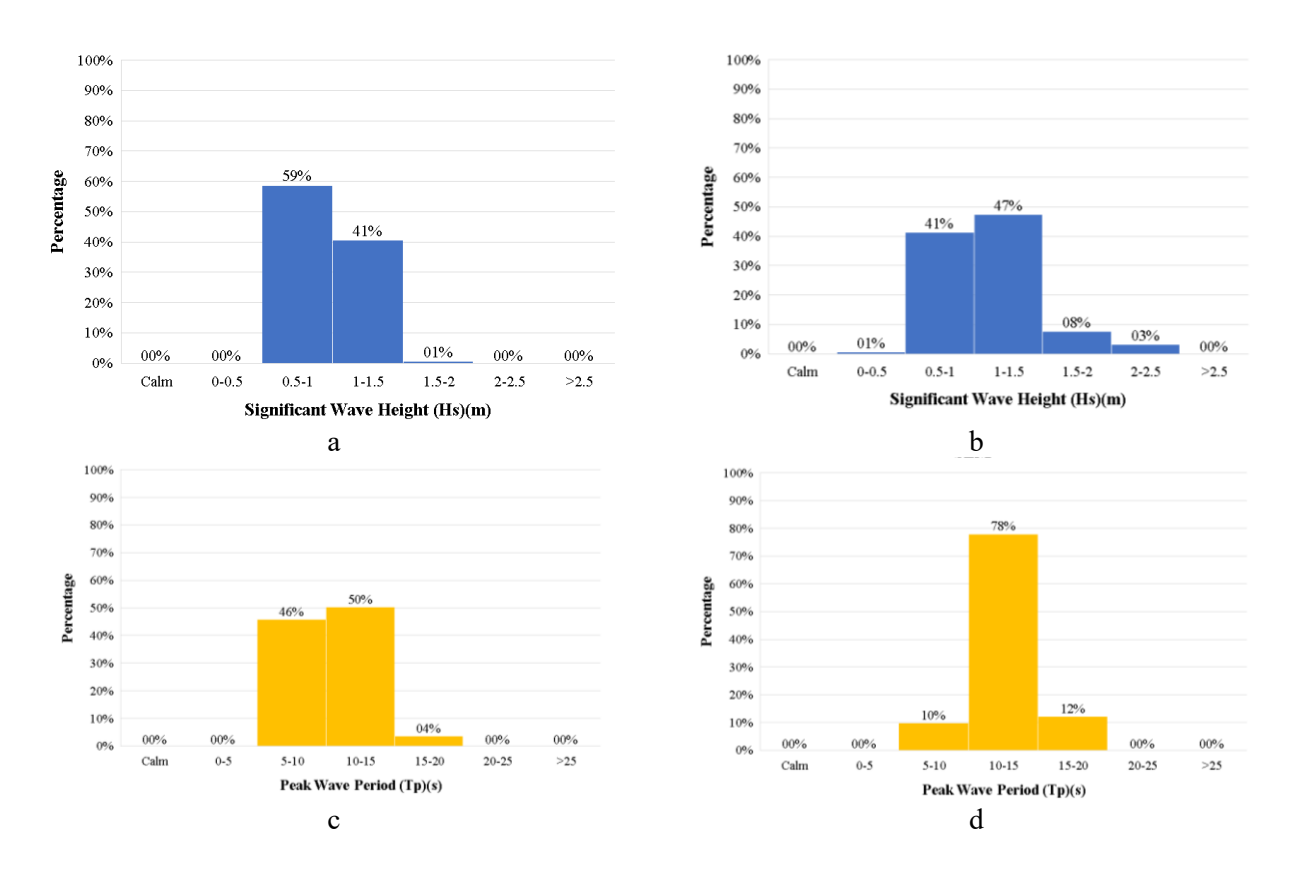


Figure 6. Seasonal histograms of H_s and T_p at the ADCP station in Cempi Bay during (a) the Northwest Monsoon (NWM) H_s , (b) Southeast Monsoon (SEM) H_s , (c) Northwest Monsoon (NWM) T_p , and (d) Southeast Monsoon (SEM) T_p .

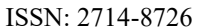
In contrast, the Southeast Monsoon (SEM) exhibited a wider and slightly higher range of H_s from 0.43 m to 2.36 m, with an average of 1.10 m. The dominant H_s bin shifted upward (Figure 6b): 1.0–1.5 m (47%) and 0.5–1.0 m (41%), with 3% of waves exceeding 2.0 m. These results confirm that SEM conditions are more energetic and variable compared to NWM, a pattern consistent with wave climatology from other Indonesian semi-enclosed bays and the Andaman Sea (Amrutha & Sanil Kumar, 2017; Anju *et al.*, 2023; Han *et al.*, 2022; Setiawan *et al.*, 2021).

Peak Wave Period

Peak wave periods during NWM spanned 5.1-18.1 s with an average of 11.01 s (Figure 6c). Two peaks emerge: swell-dominated waves at 10-15 s (50%) and locally generated wind waves at 5-10 s (46%). This bimodal pattern reflects more frequent short-period wind waves entering the bay from the west during NWM. During SEM, T_p was longer on average (13.69 s) and more strongly swell-dominated (Figure 6d), with 78% of events at 10-15 s and only 12% at 15-20 s. The scarcity of 5-10 s events in SEM indicates reduced local wind-wave generation and greater influence of remote swell entering from the south-southwest, consistent with Echevarria *et al.* (2021) and Myslenkov *et al.* (2021).

Wave Direction and Physical Mechanisms

Wave roses (Figure 7) show that during the Northwest Monsoon (NWM), waves approach mainly from the southwest and refract into the bay's entrance. Although the ADCP station is partially sheltered, the west-facing bay mouth allows local wind waves to enter, explaining the stronger presence of shorter-period waves (5–10 s). This pattern matches the histogram results in Figure 6c, where NWM conditions display a clear bimodal distribution with 46% of waves at 5–10 s and 50% at 10–15 s, reflecting the combined influence of local wind seas and incident swell. In terms of wave heights, Figure 6a shows that most NWM waves (59%) fall in the 0.5–1.0 m range, with few exceeding 1.5 m.



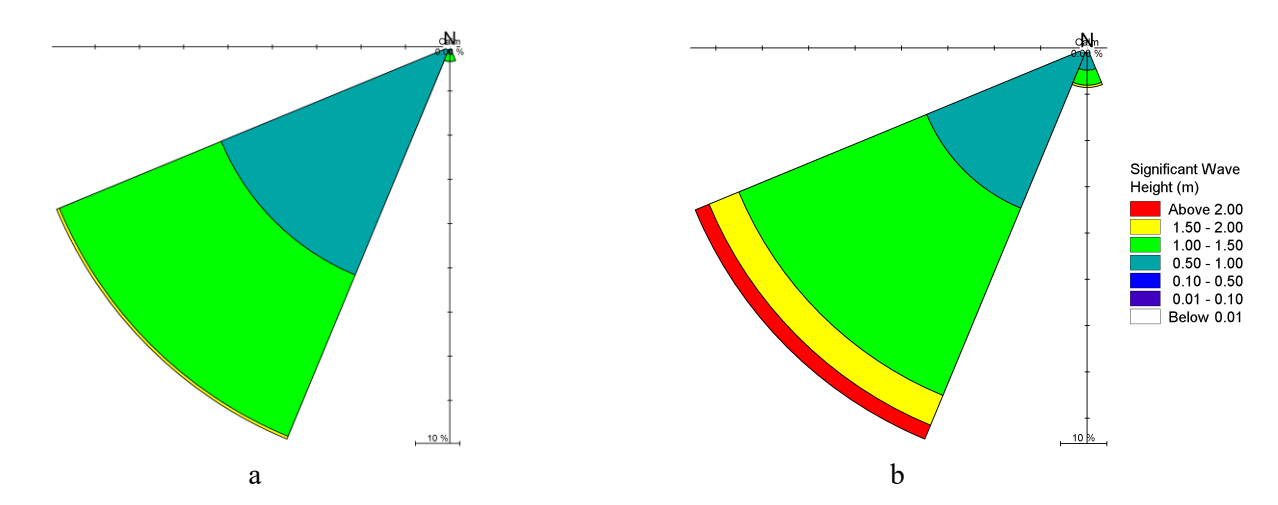


Figure 7. Wave rose diagrams of H_s at the ADCP station in Cempi Bay during (a) the Northwest Monsoon (NWM) and (b) the Southeast Monsoon (SEM).

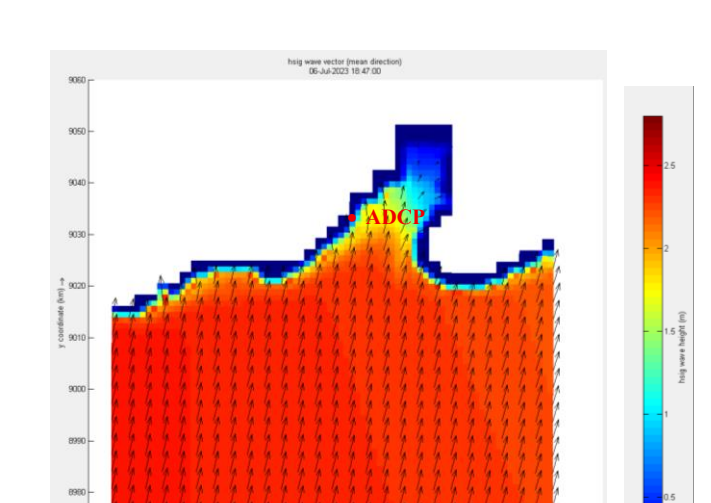
During the Southeast Monsoon (SEM), waves are predominantly from the south–southwest with higher H_S (up to > 2 m) refracted into the bay by east-side contours and a shoaling seabed. Even though the station is more protected from local winds in SEM, the persistent long-period swell (10-15 s) still penetrates deeply into the bay. This is confirmed by the histogram in Figure 6d, where 78% of SEM waves occur at 10-15 s with very few at shorter periods, indicating a swell-dominated regime. Figure 6b further shows that SEM also has a broader and slightly higher H_S distribution, with 47% of waves at 1.0–1.5 m and about 3% exceeding 2.0 m. Together these patterns demonstrate how seasonal wind fields and remote swell not only control the energy level but also the direction and period of waves reaching inner Cempi Bay. Overall, these findings highlight that Cempi Bay behaves as a semi-enclosed system strongly modulated by the interplay between local monsoon winds and remote swell propagation, a dynamic not captured in previous Indonesian regional-scale studies.

Spatial Patterns During Maximum Events

Figures 8(a and b) present the spatial distributions of H_s and wave direction during the maximum wave events. On 14 February 2023 (Northwest Monsoon, NWM), offshore H_s exceeded 2.0 m but attenuated to <1.0 m inside the embayment due to bottom friction and bathymetric sheltering. The directional vectors illustrate how NWM waves approach from the southwest at a pronounced angle to the coastline. As these waves enter the bay, they undergo strong refraction along the curved bathymetric contours and energy dissipation over shallow areas, resulting in a distinct rotation and weakening of wave energy before reaching the inner bay. On 6 July 2023 (Southeast Monsoon, SEM), the adjusted offshore H_s (79% scenario) also remained above 2.0 m, but the wave field propagated more uniformly from the south–southwest. In this case, the persistent long-period swell (10–15 s) seen in the histograms (Figure 6d) enters the bay more directly because the seasonal wind pattern aligns with the bay entrance. The east-side shoal still refracts and dissipates some energy, but overall the directional spread is narrower and the wave fronts are more parallel to the shoreline compared with NWM conditions. This reflects a more swell-dominated regime with fewer short-period wind waves and a larger proportion of high-energy waves penetrating the bay.

Both scenarios show a clear gradient of wave energy dissipation toward the inner bay (H_s <0.5 m), underscoring its relative protection from high-energy offshore waves (Karathanasi *et al.*, 2020; Portch *et al.*, 2023; Zhou *et al.*, 2023). In terms of direction, NWM waves approach obliquely and undergo stronger refraction, whereas SEM waves propagate more directly with less directional change. This spatial behaviour is consistent with the seasonal histograms and wave roses (Figures 6 and 7) and highlights the role of Cempi Bay's complex bathymetry in modulating wave transformation. The adjusted SEM scenario brings the modelled patterns much closer to the observed data, demonstrating that localized calibration improves not only the time-series agreement but also the spatial fidelity of wave transformation inside the bay. These results confirm distinct seasonal dynamics and underline the importance of high-resolution modeling for semi-enclosed tropical bays.

Diterima/Received: 28-08-2025 Disetujui/Accepted: 05-10-2025



b

ISSN: 2714-8726

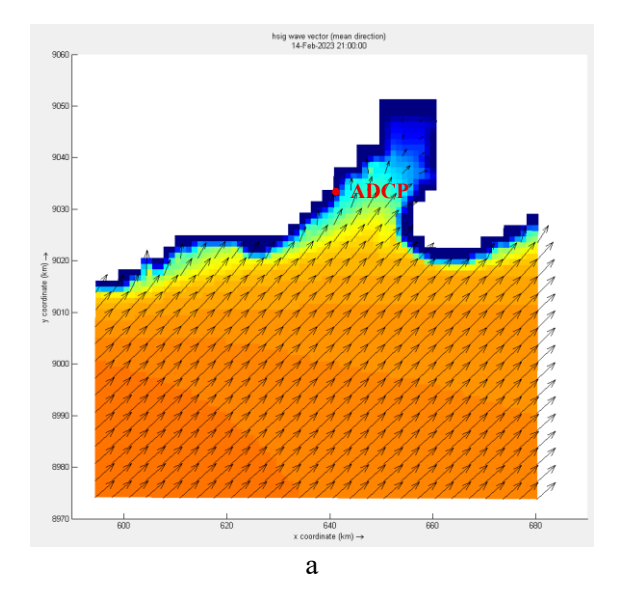


Figure 8. Wave height and direction during the maximum H_s event in the Northwest Monsoon (NWM) (a) and the adjusted H_s (79%) scenario in the Southeast Monsoon (SEM) (b) at Cempi Bay.

CONCLUSION

This study demonstrates the successful application of numerical wave modeling to characterize the seasonal hydrodynamic regime of Cempi Bay, West Nusa Tenggara, using the Delft3D-WAVE model forced by ERA5 reanalysis data and validated with in-situ ADCP measurements. The analysis reveals distinct seasonal wave characteristics between the Northwest Monsoon (NWM) and Southeast Monsoon (SEM), with mean significant wave heights of 0.97 m and 1.10 m, respectively. Model validation shows good performance during NWM (MAPE = 15.49%, R = 0.55, RMSE = 0.19 m) and improved performance during SEM following boundary condition adjustment (MAPE = 20.16%, R = 0.68, RMSE = 0.26 m). Implementing a 79% scaling factor for SEM boundary conditions reduced the initial MAPE from 42.83% to 20.16%, highlighting the critical importance of localized calibration for tropical coastal wave modeling. Spatial analyses confirm effective simulation of wave transformation, with offshore wave heights exceeding 2.0 m dissipating to below 0.5 m within the bay, reflecting the protective effects of the semi-enclosed geometry and bathymetric sheltering.

These findings substantially advance understanding of monsoon-driven wave dynamics in Indonesian coastal waters and establish a validated modeling framework applicable to similar tropical semi-enclosed systems. The study highlights the complex interplay among seasonal meteorological forcing, local bathymetry, and wave transformation processes in shaping the coastal wave climate. The predominance of swell waves (10–15 s periods) during both seasons, despite differing exposure conditions, underscores the influence of Southern Hemisphere wave generation on regional wave characteristics. Although some limitations remain, particularly in directional accuracy during transitional periods and the need for extended validation datasets, this research provides a robust basis for coastal zone management, marine infrastructure planning, fisheries activity, and disaster mitigation in the Cempi Bay region. Future work should incorporate longer-term datasets and higher-resolution wind fields, investigate extreme wave events, and extend the modeling framework to include coupled wave-current-sediment transport processes to enhance predictive capability for comprehensive coastal management.

ACKNOWLEDGEMENT

The author extends sincere appreciation to all individuals and institutions that contributed to the success of this study by providing original data and granting permission to disseminate its findings. Appreciation is also conveyed to the many others whose support and assistance were invaluable throughout the research process but cannot be acknowledged individually.

REFERENCES

Adytia, D., Saepudin, D., Tarwidi, D., Pudjaprasetya, S. R., Husrin, S., Sopaheluwakan, A., & Prasetya, G. 2023. Modelling of Deep Learning-Based Downscaling for Wave Forecasting in Coastal Area. *Water (Switzerland)*, 15(1): 204. https://doi.org/10.3390/w15010204

ISSN: 2714-8726

- Amrutha, M. M., & Sanil Kumar, V. 2017. Characteristics of high monsoon wind-waves observed at multiple stations in the eastern Arabian Sea. *Ocean Science Discussions*. pp.1-30. https://doi.org/10.5194/os-2017-84 (Preprint/Discussion paper)
- Anju, T. M., Sanil Kumar, V., Singh, J., & Bhaware, B. G. 2023. Period and length of high surface gravity waves measured in the coastal waters of eastern Arabian Sea and its variations in 10 years. *Regional Studies in Marine Science*, 67: 103224. https://doi.org/10.1016/j.rsma.2023.103224
- Baresi, E. S., Wiyono, R. U. A., & Widiarti, W. Y. 2023. Wind-Generated Wave Simulation on Payangan Beach Utilizing DELFT3D. *Proceedings of the International Conference on Sustainable Environment, Agriculture and Tourism*, pp. 619–628. https://doi.org/10.1007/978-981-16-9348-9 54
- Bitner-Gregersen, E. M., & Magnusson, A. K. 2014. Effect of intrinsic and sampling variability on wave parameters and wave statistics. *Ocean Dynamics*, 64(11): 1643–1655. https://doi.org/10.1007/s10236-014-0768-8
- De Carlo, M., & Ardhuin, F. 2024. Along-Track Resolution and Uncertainty of Altimeter-Derived Wave Height and Sea Level: Re-Defining the Significant Wave Height in Extreme Storms. *Journal of Geophysical Research: Oceans*, 129(6): e2023JC020832. https://doi.org/10.1029/2023JC020832
- Echevarria, E. R., Hemer, M. A., & Holbrook, N. J. 2021. Global implications of surface current modulation of the wind-wave field. *Ocean Modelling*, 161: 101792. https://doi.org/10.1016/j.ocemod.2021.101792
- Han, L., Ji, Q., Jia, X., Liu, Y., Han, G., & Lin, X. 2022. Significant Wave Height Prediction in the South China Sea Based on the ConvLSTM Algorithm. *Journal of Marine Science and Engineering*, 10(11): 1683. https://doi.org/10.3390/jmse10111683
- Handiani, D. N., Heriati, A., & Gunawan, W. A. 2022. Comparison of coastal vulnerability assessment for Subang Regency in North Coast West Java-Indonesia. *Geomatics, Natural Hazards and Risk*, 13(1): 1178–1206. https://doi.org/10.1080/19475705.2022.2066573
- Hanley, K. E., Belcher, S. E., & Sullivan, P. P. 2010. A Global Climatology of Wind–Wave Interaction. *Journal of Physical Oceanography*, 40(6): 1263–1282. https://doi.org/10.1175/2010JPO4377.1
- Harahap, R., Masselink, G., & Boulton, S. J. 2025. A coastal risk analysis for the outermost small islands of Indonesia: A multiple natural hazards approach. *International Journal of Disaster Risk Reduction*, 121: 105377. https://doi.org/10.1016/j.ijdrr.2025.105377
- Hünicke, B., Zorita, E., Soomere, T., Madsen, K. S., Johansson, M., & Suursaar, Ü. 2015. Recent Change—Sea Level and Wind Waves. In: *Second Assessment of Climate Change for the Baltic Sea Basin*, pp. 155–185. https://doi.org/10.1007/978-3-319-16006-1_9
- Karathanasi, F., Karperaki, A., Gerostathis, T., & Belibassakis, K. 2020. Offshore-to-Nearshore Transformation of Wave Conditions and Directional Extremes with Application to Port Resonances in the Bay of Sitia-Crete. *Atmosphere*, 11(3): 280. https://doi.org/10.3390/atmos11030280
- Mustaqim, R., Widyaningtias, W., Sekaring Bumi, I., Suryadi, Y., Oktariyanto Nugroho, E., Kardhana, H., & Bagus Adityawan, M. 2022. Hydrodynamics Analysis in Bedono Beach Demak Regency, Central Java Indonesia: Open Resource Processing for Modeling. *Jurnal Teknik Sipil*, 29(3): 217-228. https://doi.org/10.5614/jts.2022.29.3.3
- Myslenkov, S., Zelenko, A., Resnyanskii, Y., Arkhipkin, V., & Silvestrova, K. 2021. Quality of the Wind Wave Forecast in the Black Sea Including Storm Wave Analysis. *Sustainability*, 13(23): 13099. https://doi.org/10.3390/su132313099
- Portch, C. E., Cuttler, M. V. W., Buckley, M. L., Hansen, J. E., & Lowe, R. J. 2023. Wave runup and inundation dynamics on a perched beach. *Geomorphology*, 435: 108751. https://doi.org/10.1016/j.geomorph.2023. 108751
- Sagala, P. M., Bhomia, R. K., & Murdiyarso, D. 2024. Assessment of coastal vulnerability to support mangrove restoration in the northern coast of Java, Indonesia. *Regional Studies in Marine Science*, 70: 103383. https://doi.org/10.1016/j.rsma.2024.103383

ISSN: 2714-8726

- Williams, J. J., & Esteves, L. S. 2017. Guidance on Setup, Calibration, and Validation of Hydrodynamic, Wave, and Sediment Models for Shelf Seas and Estuaries. *Advances in Civil Engineering*, 2017: 5251902. https://doi.org/10.1155/2017/5251902
- Zhou, Y., Feng, X., Liu, M., & Wang, W. 2023. Influence of Beach Erosion during Wave Action in Designed Artificial Sandy Beach Using XBeach Model: Profiles and Shoreline. *Journal of Marine Science and Engineering*, 11(5): 984. https://doi.org/10.3390/jmse11050984

https://ejournal2.undip.ac.id/index.php/ijoce Diterima/Received: 28-08-2025 Disetujui/Accepted: 05-10-2025